Human Molecular Genetics, 2014, Vol. 23, No. 13 **3481–3489**
doi:10.1093/hmg/ddu056
Advance Access published on February 5, 2014

Exome sequencing identifies *de novo* gain of function missense mutation in *KCND2* in identical twins with autism and seizures that slows potassium channel inactivation

Hane Lee[1], Meng-chin A. Lin[2], Harley I. Kornblum[3,4,5], Diane M. Papazian[2] and Stanley F. Nelson[1,6,*]

[1]Department of Pathology and Laboratory Medicine, [2]Department of Physiology, [3]Department of Psychiatry, [4]Department of Molecular and Medical Pharmacology, [5]Department of Pediatrics and [6]Department of Human Genetics, University of California, Los Angeles, CA 90095, USA

Received November 22, 2013; Revised and Accepted January 31, 2014

Numerous studies and case reports show comorbidity of autism and epilepsy, suggesting some common molecular underpinnings of the two phenotypes. However, the relationship between the two, on the molecular level, remains unclear. Here, whole exome sequencing was performed on a family with identical twins affected with autism and severe, intractable seizures. A *de novo* variant was identified in the *KCND2* gene, which encodes the Kv4.2 potassium channel. Kv4.2 is a major pore-forming subunit in somatodendritic subthreshold A-type potassium current (I_{SA}) channels. The *de novo* mutation p.Val404Met is novel and occurs at a highly conserved residue within the *C*-terminal end of the transmembrane helix S6 region of the ion permeation pathway. Functional analysis revealed the likely pathogenicity of the variant in that the p.Val404Met mutant construct showed significantly slowed inactivation, either by itself or after equimolar coexpression with the wild-type Kv4.2 channel construct consistent with a dominant effect. Further, the effect of the mutation on closed-state inactivation was evident in the presence of auxiliary subunits that associate with Kv4 subunits to form I_{SA} channels *in vivo*. Discovery of a functionally relevant novel *de novo* variant, coupled with physiological evidence that the mutant protein disrupts potassium current inactivation, strongly supports *KCND2* as the causal gene for epilepsy in this family. Interaction of *KCND2* with other genes implicated in autism and the role of *KCND2* in synaptic plasticity provide suggestive evidence of an etiological role in autism.

INTRODUCTION

Inherited seizure disorders are caused by abnormal regulation of membrane excitability. While the genetic basis of epilepsy is highly heterogeneous, the most common genes in which mutations lead to a seizure disorder encode ion channels that mediate the axonal conduction of action potentials and signal transduction through synaptic transmission (1,2). To date, autosomal dominant mutations in *KCND2* have not been identified to cause epilepsy. Autism spectrum disorder (ASD), another early-onset disorder with a high prevalence of ∼1.1% (3), has been widely demonstrated to be heritable, but is also highly complex. Several large-scale genome-wide association studies have resulted in few strong common allele associations. Thus, with the advent of more powerful sequencing technology, attention has shifted to considering ASD as many independent rare monogenic disorders, and much effort is being made to identify *de novo* variants in ASD population (4–8). In many of the cases, rare *de novo* variants in ASD cases are identified in a single subject, and independent mutations in additional ASD cases are needed to determine causality. Both epilepsy and ASD are commonly associated with other phenotypes and co-occurrence of autism and epilepsy has been well documented. Recent reports show that 15–35% of children with epilepsy also present with ASDs and 7–46% of ASD patients are affected with epilepsy (9–14). Several candidate genes have been implicated as causal for the observed comorbidity of ASD and epilepsy, but none are conclusive (15).

* To whom correspondence should be addressed. Tel: +1 3107947981; Fax: +1 3107945446; Email: snelson@ucla.edu

Potassium channel genes are one of the largest groups of genes that have been implicated for epilepsy and seizures and also one of the most widely distributed types of ion channels that shapes the action potential and sets the resting membrane potential. Shal-type K^+ channels, Kv4.x, are expressed throughout the brain, heart and smooth muscles. Each isoform, Kv4.1, Kv4.2 and Kv4.3, has different expression patterns, with Kv4.2 being the predominant isoform in some of the specific brain areas such as hippocampus CA1 pyramidal cells, dentate gyrus granule cells, habenula and cerebellum granule cell layer anterior lobules (2). In neurons, Kv4 proteins serve as the pore-forming subunits in inactivating somatodendritic subthreshold A-type potassium current (I_{SA}) channels that regulate the rate of low-frequency firing and control backpropagation of action potentials into the dendritic tree (16). The availability of I_{SA} channels, which is determined by the extent of inactivation, reflects the recent history of activity in the cell. Inactivation is therefore essential for regulating the physiological functions of I_{SA} (16). I_{SA} channels exhibit at least two types of inactivation (16,17). Kv4 channels can inactivate from the open state using an *N*-type mechanism in which the open pore is plugged by an *N*-terminal inactivation domain (18). However, this form of inactivation is unstable in Kv4 channels and probably does not contribute significantly to the steady-state availability of I_{SA} channels in neurons. Kv4 channels also inactivate from preopen closed states when the voltage sensor domains activate but the pore fails to open (17,19,20). This is the predominant form of Kv4 inactivation.

Here we report a whole exome sequencing discovery of a novel *de novo* heterozygous variant in *KCND2* gene in identical twin patients with autism and epilepsy (Fig. 1A) and demonstrate that this variant leads to altered electrophysiology *in vitro* with impaired closed-state inactivation. Based on this finding, taken together with previous reports on the role of Kv4.2 channel in synaptic plasticity, and that other components of the Kv4.2 channel are associated with autism, we propose that *KCND2* is the causal gene for epilepsy in this family and has a role in the etiology of autism.

RESULTS

Patient clinical information

The monozygotic twins affected with seizures and autism (Fig. 1A) were born at 35 weeks gestation without complication and began to have seizures at 2 months of age, consisting of brief jerks of the extremities. Over the course of the first decade of life, the seizures were uncontrolled, occurring up to many hundreds per day, despite trials of multiple medications and the ketogenic diet. Diagnostic evaluations included MRI scans and metabolic testing, which were unremarkable. An electroencephalography performed in the first year of life demonstrated 3–4 Hz poly spike and wave by report. As the patients grew older, the seizures consisted of both staring spells as well as generalized convulsions. Between 8 and 10 years of age, the seizures decreased in frequency, with the parents reporting that generalized convulsions were occurring less than weekly, and staring spells occurring somewhat more frequently. The subjects have had no significant other medical problems with repeated normal physical examinations. Their head circumference is approximately the 95th percentile for age. At the age of 15, the subjects underwent detailed evaluation to determine whether the diagnosis of autism was appropriate and to evaluate their cognitive development. To assess autism, they (and parents) were administered Autism Diagnostic Interview–Revised (21) and the Autism Diagnostic Observation Schedule–2, Module 1 (22). Both subjects met criteria for ASD, based on the *DSM-V* (*Diagnostic and Statistical Manual of Mental Disorders, 5th Edition*) (23). Owing to their limited verbal abilities, the subjects were administered the Mullen Scales of Early Learning (24) to obtain an estimate of their cognitive functioning. Both exhibited overall cognitive functioning in the 'Very Low' range. Twin 1 had expressive language estimated at the level of 4 months of age, and receptive language was equivalent to 11 months. Twin 2 had expressive language estimated at 9 months of age, and receptive language was equivalent to 16 months.

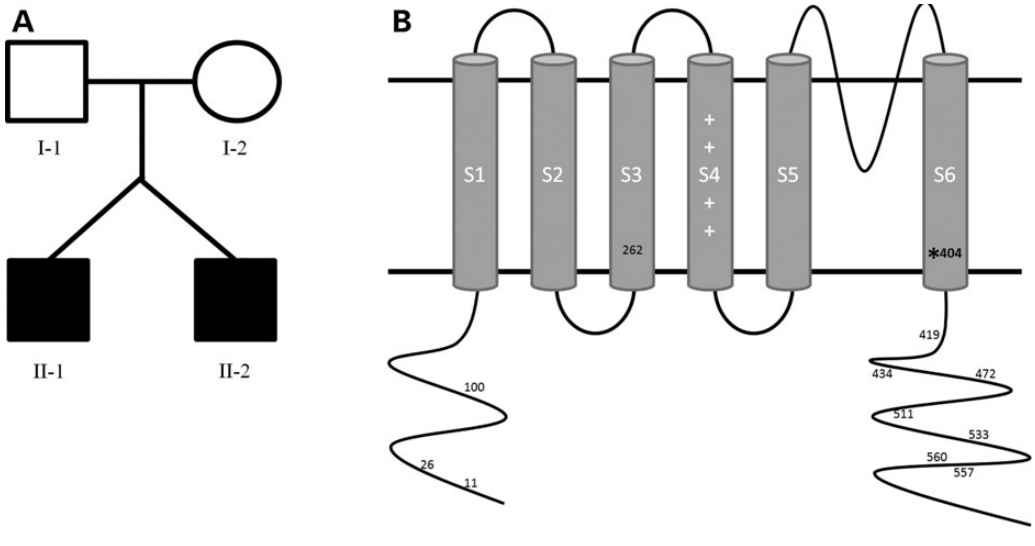

Figure 1. (**A**) Pedigree of the family. (**B**) Amino acid positions where predicted-to-be-damaging (probably damaging or possibly damaging by PolyPhen) missense variants are found in the population (exome variant server) are indicated. The *404 position is where the *de novo* variant was found.

Table 1. Summary of rare protein-altering variants identified to be shared between the two affected identical twins

Gene	Genomic position (hg19)	Inheritance	Zygosity	DNA change	Protein change	MAF in EVS[a]
KCND2	7:120373051	*De novo*	Heterozygous	NM_012281.2:c.1210G>A	p.Val404Met	0%
BICC1	10:60549454	*De novo*	Heterozygous	NM_001080512.1:c.808A>G	p.Met270Val	0%
SLC8A2	19:47944606	Maternal	Heterozygous	NM_015063.2:c.1855C>T	p.Arg619[a]	0%
SLC8A2	19:47969575	Paternal	Heterozygous	NM_015063.2:c.86C>T	p.Pro29Leu	0%
GPR124	8:37688966	Paternal	Heterozygous	NM_032777.9:c.958G>A	p.Val320Met	0.87%
GPR124	8:37699298	Maternal	Heterozygous	NM_032777.9:c.3442G>T	p. Glu1148[a]	0%

[a]MAF in EVS: Minor allele frequency in exome variant server.

Whole exome sequencing

Two *de novo* variants in the *KCND2* and *BICC1* genes were identified, and two sets of compound heterozygous variants were identified in the *SLC8A2* gene and the *GPR124* gene (Table 1). No rare homozygous or hemizygous variants were identified, and no large intervals of homozygosity were identified. Except for one variant in the *GPR124* gene, all variants were novel, not observed in the ∼6500 exome variant server (EVS, http://eversusgs.washington.edu/EVS/), or in an internal database from the UCLA Clinical Genomics Center consisting of 700 exomes.

SLC8A2 gene, in which the affected twins have compound heterozygous variants, encodes one of the three isoforms of the plasma membrane Na^+/Ca^+ exchanger (NCX), NCX2. *SLC8A2* has not been associated with any human disease or phenotype yet. However, NCX2 is reported to be restrictively expressed in hippocampus, cerebellum and cortex, and knockout mice showed enhanced learning and memory capacity (25). Variants in *BICC1* are associated with cystic renal dysplasia in humans (26), and mouse mutations in Bicc1 result in polycystic kidneys (27), which our patients do not manifest. The *de novo* variant found in *KCND2* gene replaces valine for methionine at amino acid 404 (p.Val404Met) and is predicted to be 'deleterious', 'probably damaging' and 'deleterious' by SIFT, PolyPhen-2 and Condel, respectively. The conservation score measured by GERP was 5.41, and valine is highly conserved across 41 vertebrates. This variant is found at the *C*-terminal end of the transmembrane helix S6 region (amino acid 385–405, Fig. 1B) that makes up the ion permeation pathway along with the S5 domain and the P-loop (28). The six transmembrane domains of Kv4.2 are in general depleted of predicted-to-be-damaging variants in EVS, suggesting that variation is not well tolerated in these regions (Fig. 1B). One prior frameshift mutation (p.Asn587fs*1) in *KCND2* was reported in a child with temporal lobe epilepsy. However, the unaffected father of the patient was a carrier of the same frameshift mutation. The affected proband was not reported to have autism.

P.Val404Met mutation dominantly impairs closed-state inactivation

As the *de novo* heterozygous variant in *KCND2* was the most plausible variant related to the seizure disorder, we further investigated the functional consequence of the p.Val404Met mutation on Kv4.2 channels *in vitro* by expressing wild-type and mutant proteins in Xenopus oocytes (Fig. 2) (29,30). Ionic currents were evoked by depolarizing from a holding potential of −100 mV to voltages ranging from −80 to +70 mV. Potassium current through wild-type Kv4.2 channels was first detected at −50 mV (Fig. 2A). At more depolarized voltages, the rate of opening and peak current amplitude increased, and inactivation became more obvious. Similarly, K^+ current through mutant p.Val404Met channels was first detected at −50 mV (Fig. 2A). However, at more depolarized voltages, p.Met404 currents reached their peak amplitude significantly later than p.Val404 (Figs 2A and B and 3A), and the decay of the current was significantly slower and less complete. As a result, the ratio of current amplitude at the end of the pulse relative to the peak current amplitude was significantly increased in mutant channels compared with wild-type channels (Figs 2A and B and 3A). Because the time to peak reflects the competing processes of opening and inactivation, changes in the time course of inactivation are likely responsible for the effect of the p.Val404Met mutation on the time to peak.

The genomes of the affected twins contain one wild-type and one mutant *KCND2* allele. Because potassium channels are tetramers of pore-forming subunits (31), p.Val404 and p.Met404 subunits are expected to coassemble into functional heterotetramers. To characterize the functional properties of channels containing both types of subunits, p.Val404 and p.Met404 were coexpressed at a 1:1 ratio (Fig. 2A). Both RNAs made active channel proteins with no significant difference in expression level. The resulting currents resembled those obtained when the p.Met404 protein was expressed alone, reaching peak current amplitude significantly later and inactivating more slowly and less completely than p.Val404 channels (Fig. 2A and B). These results indicate that the functional effects of the p.Val404Met mutation are dominant, consistent with the family pedigree and heterozygous genotype.

In vivo, Kv4 pore-forming subunits associate with auxiliary subunits, including members of the K^+ channel interacting protein (KChIP) and dipeptidyl-peptidase-like protein (DPP) families (32,33). These auxiliary subunits modulate the functional properties of Kv4 channels to more closely resemble native I_{SA} currents. KChIP and DPP subunits have differential effects on Kv4 inactivation. KChIP subunits bind to the cytoplasmic N-terminal domain of Kv4 subunits and prevent or greatly inhibit N-type open-state inactivation (34). In contrast, DPP10a and DPP6a subunits confer fast, open-state inactivation via their N-terminal domains, which insert into the cytoplasmic end of the open pore, preventing conductance (35). To determine the effect of the p.Val404Met mutation in the presence of auxiliary subunits, p.Val404 or p.Met404 were coexpressed with KChIP3a or DPP10a by injecting RNA encoding KChIP3a or DPP10a at a 1:1 molar ratio (32) (Fig. 2C–F). In addition, a 1:1

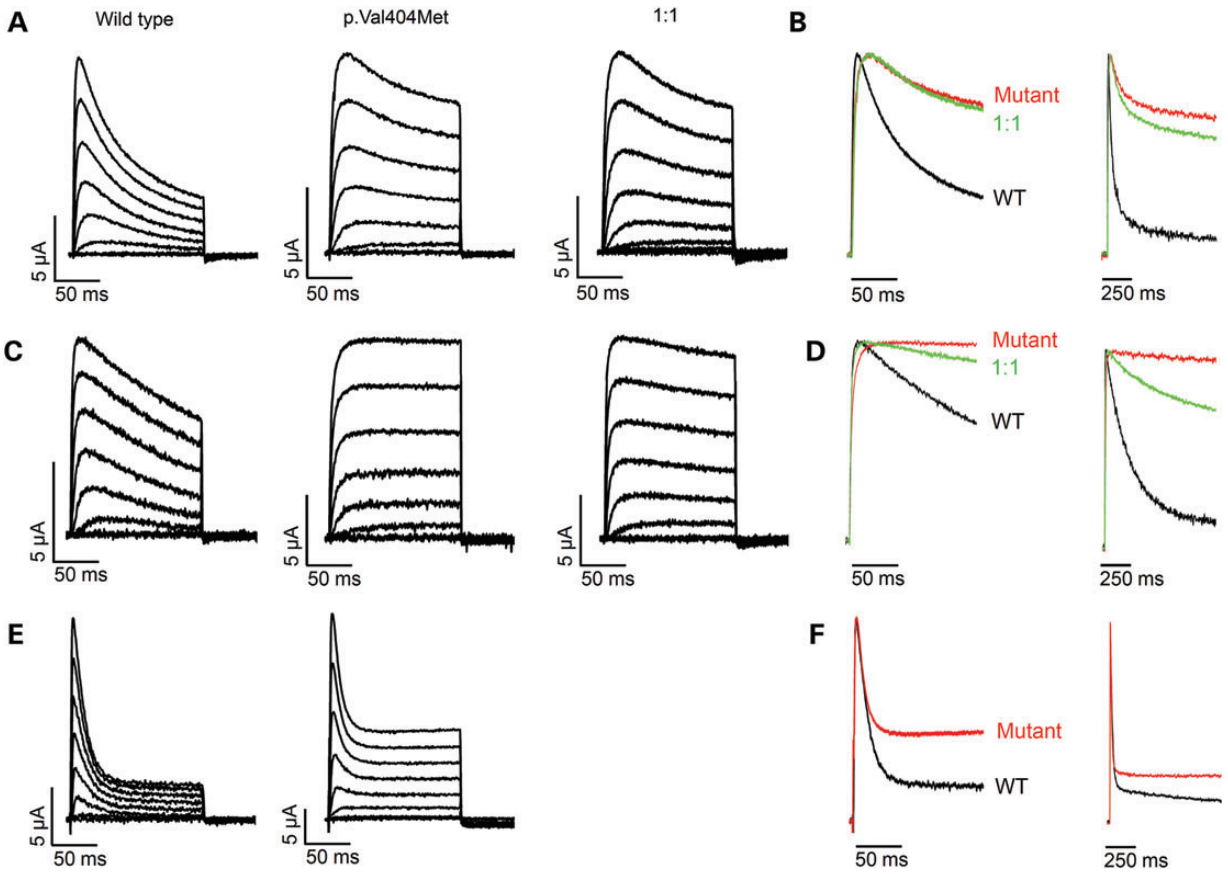

Figure 2. p.Val404Met mutation impairs closed-state inactivation in Kv4.2 channels. (**A**, **C** and **E**) Representative current traces were recorded in Xenopus oocytes after expressing wild-type Kv4.2 (left), the p.Val404Met mutant protein (middle), or a 1:1 mixture of wild-type and mutant (right) in the A) absence or presence of the C) KChIP3a or E) DPP10a auxiliary subunits. Currents were evoked by pulsing for 150 ms from a holding potential of −100 mV to voltages ranging from −80 to +70 mV in 10 mV increments. For clarity, only every other trace is shown. (**B**, **D** and **F**) Current traces evoked at +60 mV have been scaled and overlaid after expressing wild-type Kv4.2 (WT, black), the p.Val404Met mutant protein (mutant, red), or a 1:1 mixture of wild-type and mutant (1:1, green) in the B) absence or presence of the D) KChIP3a or F) DPP10a auxiliary subunits. Pulse durations of 150 ms (left) and 1 s (right) are shown.

mixture of p.Val404 and p.Met404 was coexpressed with KChIP3a (Fig. 2C and D). As previously reported, KChIP3a slowed the rate and decreased the extent of current decay in wild-type channels (Figs 2C, D and 3B) (32,36). When KChIP3a was incorporated with p.Met404 channels, little inactivation occurred during pulses lasting for 150 ms or 1 s (Figs 2C, D and 3B). When KChIP3a was incorporated into channels formed from a mixture of wild-type and mutant subunits, macroscopic current decay was somewhat faster than in mutant channels, resulting in a greater extent of inactivation (Figs 2C and D and 3B). The time to reach the peak current amplitude was correlated with the rate and extent of inactivation (Figs 2D and 3B). Wild-type channels reached their peak current amplitude significantly faster than p.Met404 channels, whereas mixed p.Val404/p.Met404 channels had an intermediate value (Fig. 3B). These results indicate that the p.Val404Met mutation significantly impairs closed-state inactivation, which is the main form of inactivation that occurs in the presence of KChIP3a (19).

When p.Val404 or p.Met404 was coexpressed with DPP10a, a fast component of inactivation conferred by the auxiliary subunit was observed (Fig. 2E and F) (35). Fast inactivation decreased the time to peak current amplitude, which did not differ significantly between wild-type and mutant channels (Fig. 3C). However, the effect of the p.Val404Met mutation on closed-state inactivation was still evident because the ratio of current amplitude at the end of the pulse relative to the peak current amplitude was significantly greater than in wild-type channels (Figs 2F and 3C). These results indicate that the p.Val404Met mutation does not interfere with open-state inactivation conferred by the DPP10a subunit and that DPP10a does not mask the aberrant effect of p.Met404 on closed-state inactivation kinetics.

DISCUSSION

Our results indicate that the substitution mutation, p.Val404Met, profoundly impairs closed-state inactivation when the mutant protein is expressed alone or in combination with wild-type Kv4.2. The effect of the mutation on closed-state inactivation is evident in the presence of the KChIP3a or DPP10a auxiliary subunits, which associate with Kv4 subunits to form I_{SA} channels *in vivo* (33). Our results are compatible with previous reports implicating p.Val404 in Kv4.2 and the equivalent residues p.Val406 and p.Val401 in Kv4.1 and Kv4.3, respectively, in the mechanism of closed-state inactivation (20,34,37). Closed-state inactivation in Kv4 channels is thought to involve

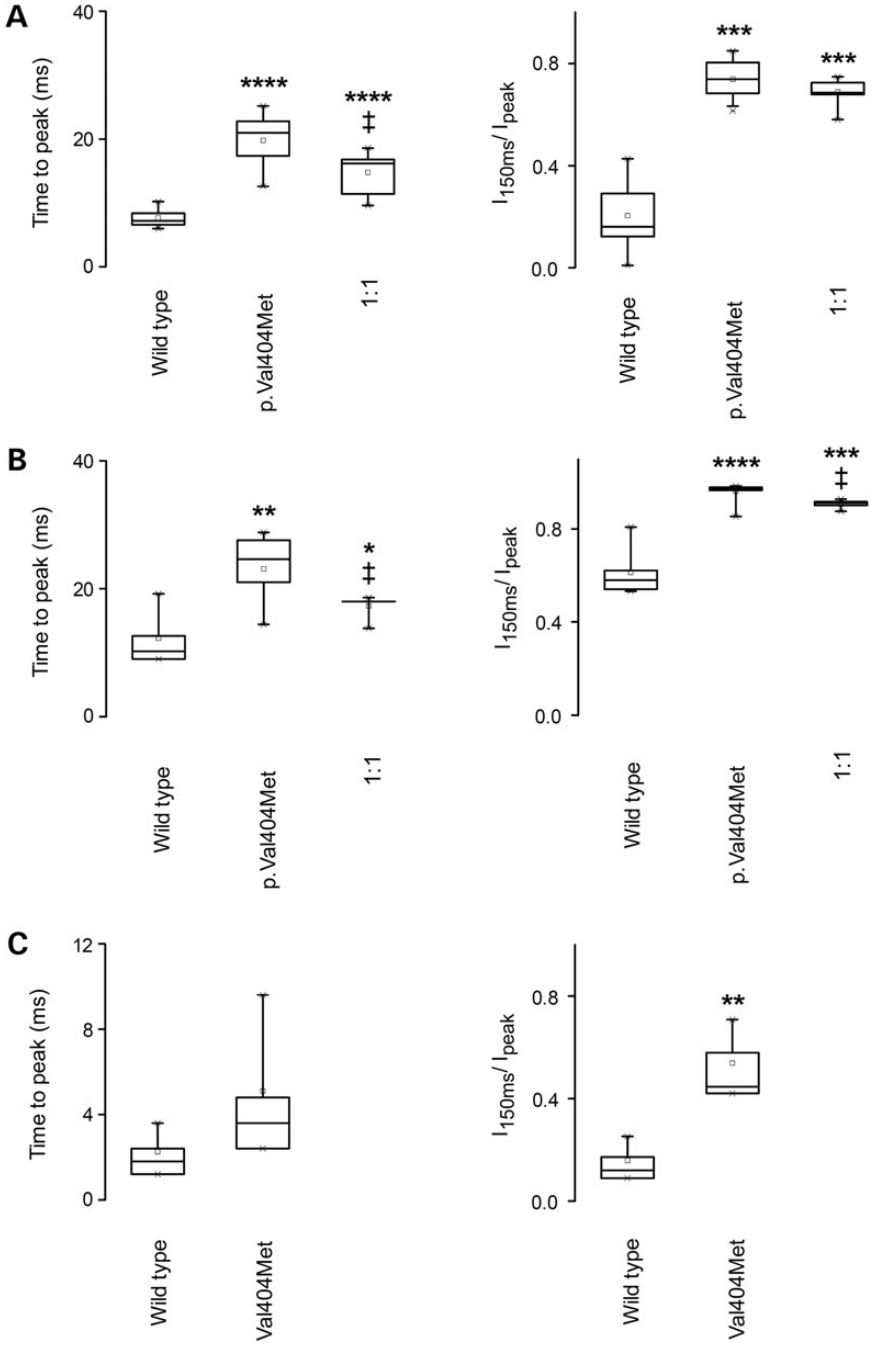

Figure 3. p.Val404Met mutation slows time to reach peak current amplitude and increases amplitude of current remaining at end of pulse. The box plots show the time to reach peak current amplitude at +60 mV (left panels) and the ratio of current amplitude at the end of a 150 ms pulse relative to the peak current amplitude measured at +60 mV (I_{150ms}/I_{peak}, right panels) after expressing wild-type Kv4.2, the p.Val404Met mutant protein, or a 1:1 mixture of wild-type and mutant (1:1) in the (**A**) absence or presence of the (**B**) KChIP3a or (**C**) DPP10a auxiliary subunits. The mean time to peak values (ms) ± SEM were: (A) wild-type, 7.7 ± 0.4 ($n = 14$); p.Val404Met, 19.8 ± 1.0 ($n = 17$); 1:1 mixture, 14.8 ± 1.4 ($n = 6$); (B) wild-type, 12.2 ± 1.3 ($n = 8$); p.Val404Met, 23.1 ± 1.7 ($n = 9$), 1:1 mixture, 17.3 ± 0.9 ($n = 5$); and (C) wild-type, 2.3 ± 0.5 ($n = 4$); p.Val404Met, 5.1 ± 1.6 ($n = 4$). The mean values of I_{150ms}/I_{peak} ± SEM were: (A) wild-type, 0.25 ± 0.02 ($n = 11$); p.Val404Met, 0.74 ± 0.02 ($n = 21$), and 1:1 mixture, 0.69 ± 0.02 ($n = 6$); (B) wild-type, 0.61 ± 0.03 ($n = 8$); p.Val404Met, 0.96 ± 0.01 ($n = 9$); 1:1 mixture, 0.91 ± 0.01 ($n = 5$); and C) wild-type, 0.16 ± 0.04 ($n = 4$); p.Val404Met, 0.54 ± 0.10 ($n = 4$). Statistical significance was evaluated by one-way ANOVA followed by Student's *t*-test: $^{****}P < 0.00001$ compared with wild-type alone; $^{***}P < 0.0005$ compared with wild-type alone; $^{**}P < 0.005$ compared with wild-type alone; $^{*}P < 0.05$ compared with wild-type alone; ‡, $P < 0.05$ compared with p.Val404Met alone.

uncoupling between the voltage sensor domains and the cytoplasmic gate that closes the pore. Mechanical coupling is provided by residues in the linker between transmembrane segments S4 and S5. In response to depolarization, conformational changes in the voltage sensor domain pull on the gate, causing the S6 helices to splay apart by bending at a well-conserved sequence

Pro–Val–Pro–Val corresponding to residues 401–404 in Kv4.2 (38). In Kv4.2 channels, interactions between p.Val404 in S6 and residues in the S4–S5 linker, particularly Glu323 at the cytoplasmic end of S5, maintain the coupling between the gate and the sensor (20). Because p.Val404 is a pivotal residue in gate–sensor interactions, mutations at this position profoundly affect closed-state inactivation, as we observe in channels bearing the mutation found in this family (19).

Our results taken together with previous reports strongly suggest that the size of the residue at position 404 is a major factor in determining the likelihood of inactivation. For instance, mutations p.Val404Ala and p.Val406Ile at the equivalent position in Kv4.1 have opposite effects on closed-state inactivation rate (20,37). Replacing valine (mean volume in protein = 139.1 $Å^3$) (39) by the smaller alanine residue (90.1 $Å^3$) enhances closed-state inactivation, perhaps because the smaller residue weakens the (already-weak) coupling between position 404 and residues in the S4–S5 linker, increasing the likelihood of sensor–gate uncoupling (20). In contrast, replacing valine by the larger isoleucine residue (164.9 $Å^3$) impairs closed-state inactivation perhaps because the larger residue is better able to maintain the physical interaction between the gate and the voltage sensor domain so that opening is preferred over closed-state inactivation (37). Methionine (167.7 $Å^3$) is similar in size to isoleucine, consistent with our results showing greatly decreased closed-state inactivation in the presence of the p.Val404Met mutation (39). Given the key role of closed-state inactivation in determining the steady-state availability of I_{SA} channels in neurons, the dominant phenotype of p.Val404Met is likely to disrupt the normal physiological functions of $I_{SA.}$ Reduced inactivation (increased K^+ currents) because of the p.Val404Met mutation would be expected to decrease excitability, which, in GABAergic neurons, could lead to the observed seizure disorder through disinhibition.

While the specific *KCND2* mutation identified here is not clearly demonstrated to be causal of ASD, we note that several links can be made between Kv4.2 mutations and ASD. First, rare variants in *KCND2* have been previously identified in individuals with autism including a submicroscopic *de novo* deletion encompassing *KCND2* (40), three translocation breakpoints at 7q22.1, 7q31.2 and 7q31.3 potentially disrupting *KCND2* (41), and three substitution variants, p.Asn544Ser, p.Phe538Ser and p.Arg539Leu. The three substitution variants were found in the C-terminal intracellular portion of *KCND2* and were reported in three independent autism cases (42). Based on PolyPhen-2/SIFT, these three variants are predicted to be benign/tolerated, benign/tolerated and possibly damaging/tolerated, respectively. However, all three amino acid positions are completely conserved in primates, mouse and rats. *KCND2* is located within a recently identified interval of enriched homozygous haplotype shared within a large ASD cohort (43). Secondly, DPP6 and DPP10 proteins are auxiliary subunits of Kv4.2. These DPP proteins interact with the transmembrane domains of Kv4 proteins, and confer fast inactivation of the channel. Although no point mutations have been reported for *DPP6* and *DPP10* in ASD or epilepsy cases, each of these genes has been repeatedly reported within copy number variants in autism cases (44,45). Further, loss of function variants in DPP proteins are predicted to slow channel inactivation similar to the functional consequence of V404M observed here. Thirdly, Fragile X syndrome is one of the leading single-gene disorders associated with ASD, accounting for up to 5% of the ASD cases (46). Kv4.2 is highly expressed in the cell bodies and along the dendrites of hippocampal neurons, and the fragile X mental retardation protein (FMRP), which is itself regulated by a transmitter receptor metabotropic glutamate receptor (mGluR), interacts directly with Kv4.2–3′UTR to suppress Kv4.2 translation (47). When FMRP is knocked out, the expression level of Kv4.2 increases compromising synaptic plasticity (47). Notably, a significant overlap between FMRP target genes and genes mutated in ASD individuals has been observed (48). In hippocampus CA1 pyramidal cells, Kv4.2 expression determines synapse maturational state (49). Lastly, recent data and network-based gene expression analysis indicate that *KCND2* mRNA is coexpressed in developing human cortex with other autism-implicated genes within a module related to synaptic development (M17 in Parikshak *et al.*) (50). Further, data from fetal human and adult primate laminae show that *KCND2* is preferentially expressed in the outer cortical plate of fetus and adult L2, suggesting Kv4.2 dysfunction may preferentially affect upper cortical layer neurons further linking the variant to autism phenotype. *KCND2* expression pattern in adult correlates highly with GABAergic markers, further suggesting that it may play a role in this cell type. From the combination of all of the above data, it is highly plausible that the specific mutation identified here has directly contributed to a defect in synaptic homeostasis and the severe autism phenotype.

In conclusion, we identified a *de novo* variant p.Val404Met in *KCND2* using whole exome sequencing in a family with atypical autism and severe, intractable epilepsy. The non-synonymous *de novo* variant p.Val404Met identified in *KCND2* gene is a previously studied residue that plays a critical role in both voltage-dependent gate opening and closed-state inactivation, and has been suggested to be involved in a dynamic coupling between the voltage sensor and the cytoplasmic gate to mediate the inactivation of Kv4.2 channels (20). Although without an *in vivo* model of *KCND2* mutation, we cannot exclude that other variants, especially the ones that were identified in *de novo* or compound heterozygous states in *BICC1*, *SLC8A2* and *GPR124*, may contribute some effect to the complex phenotype of epilepsy and autism, we believe that these data in aggregate strongly implicate that mutations in *KCND2* can cause epilepsy and autism. Also, a number of reports showing essential proteins interacting with Kv4.2 being implicated in autistic features provide suggestive evidence of Kv4.2 playing a role in autism even though *KCND2* has not been reported in any of the recent exome sequencing studies (4–6,8) implying that autism cases explained by *KCND2* mutations will be extremely rare.

MATERIALS AND METHODS

Whole exome sequencing

After institutional review board-approved informed consent, blood was obtained from participating family members: the unaffected parents and the affected identical twins. Genomic DNA was extracted using standard methods (QIAcube Qiagen, Valencia, CA, USA) at the UCLA Orphan Disease Testing Center. Library preparation, sequencing and data analysis were performed at the UCLA Clinical Genomics Center using the CLIA- (Clinical Laboratory Improvement Amendments) and CAP (College of American Pathologists)-validated protocols. An amount of 3 μg of

high-molecular-weight genomic DNA from each participant was subjected to library preparation and exome capture following the Agilent SureSelect Human All Exon 50 Mb Illumina Paired-End Sequencing Library Prep Protocol. Sequencing was performed on an Illumina HiSeq2000 as a 50 bp paired-end run. For each sample, ~200 million independent paired reads were generated for an average coverage of 140× of RefSeq protein coding exons and flanking introns (±2 bp) with ~95% of these bases covered at ≥10×. The sequences were aligned to the hg19/b37 genome release using Novoalign. PCR duplicates were marked using Picard. GATK was used for indel realignment and base quality recalibration. Both SNVs (single nucleotide variants) and small INDELs (insertions and deletions) were called using GATK unified genotyper (51,52). All variants were annotated using the customized VEP (variant effect predictor) engine from Ensembl. Linkdatagen (53,54) and PLINK (55) determined regions of homozygosity by descent. A total of 21 890 variants were shared between the two affected identical twins, and rare protein-altering variants were examined under different inheritance models.

Electrophysiology study

We obtained the full-length human *KCND2* cDNA in pCR-Blunt II-TOPO (clone Id 40012007) from Thermo Scientific Open Biosystems (Waltham, MA, USA). The mutation was introduced into the reference sequence construct using QuikChange II XL Site-Directed Mutagenesis Kit (Agilent Technologies, Santa Clara, CA, USA).

Plasmid cDNA clones of human *KChIP3a* (pT3T7–hKChIP3a) and *DPP10a* (pBSR–hDPP10a) were kindly provided by Dr Paul J. Pfaffinger, Baylor College of Medicine (32). RNA was transcribed *in vitro* using the mMessage mMachine T7 Ultra kit (Ambion, Life Technologies, Grand Island, NY, USA) and injected into Stage V–VI oocytes from Xenopus laevis. All animal procedures were approved by the Chancellor's Animal Research Committee at the University of California, Los Angeles.

Ionic currents were recorded in oocytes 1–3 days after RNA injection using a Warner OC-725 two-electrode voltage clamp (29,30). Electrodes were filled with 3 M KCl and had resistances ranging from 0.3–1.0 MΩ. The bath solution contained 2 mM KCl, 96 mM NaCl, 0.5 mM $CaCl_2$, and 5 mM HEPES, pH 7.5. The functional properties of wild-type (p.Val404), mutant (p.Met404), and mixed wild-type/mutant channels were investigated in the presence or absence of KChIP3a or DPP10a using standard pulse protocols as described in the figure legends. Linear leak and capacitive currents were subtracted using a P/−4 protocol.

WEB RESOURCES

Online Mendelian Inheritance in Man (OMIM), http://www.ncbi.nlm.nih.gov/Omim (accessed on 10 February 2014).

Novocraft Short Read Alignment Package, http://www.novocraft.com (accessed on 10 February 2014).

Genome Analysis Toolkit, ftp://gsapubftp-anonymous@ftp.broadinstitute.org (accessed on 10 February 2014).

SAMtools, http://samtools.sourceforge.net/ (accessed on 10 February 2014).

Picard, http://picard.sourceforge.net/ (accessed on 10 February 2014).

PolyPhen-2, http://genetics.bwh.harvard.edu/pph2/bgi.shtml (accessed on 10 February 2014).

SIFT, http://sift.jcvi.org/ (accessed on 10 February 2014).

Exome Variant Server, NHLBI Exome Sequencing Project (ESP), Seattle, WA, http://evs.gs.washington.edu/EVS/ (accessed on 10 February 2014).

Human Reference Genome: ftp://ftp.1000genomes.ebi.ac.uk/vol1/ftp/technical/reference/ (accessed on 3 September 2013).

ACKNOWLEDGEMENTS

Technical work for sequencing was performed by Jean Reiss and Traci Lyn Toy. Computational support for sequence data analysis was provided by Bret Harry. Variant annotation was assisted by programs developed by Paige Taylor. We acknowledge Jieun Hong and Dr Joanna Jen for assisting with the mutagenesis and subcloning. We thank Dr Paul J. Pfaffinger (Baylor College of Medicine) for human KChIP3a and DPP10a clones.

Conflict of Interest statement. None declared.

FUNDING

The work was performed within the UCLA Clinical Genomics Center with support from the P30 UCLA Muscular Dystrophy Core Center grant to S.N., National Institutes of Health grant 5R01NS073871-03 to S.N. and National Institutes of Health grant 5R01GM043459-21 to D.M.P.

REFERENCES

1. Lerche, H., Jurkat-Rott, K. and Lehmann-Horn, F. (2001) Ion channels and epilepsy. *Am. J. Med. Genet.*, **106**, 146–159.
2. Serodio, P. and Rudy, B. (1998) Differential expression of Kv4 K+ channel subunits mediating subthreshold transient K+ (A-type) currents in rat brain. *J. Neurophysiol.*, **79**, 1081–1091.
3. Perou, R., Bitsko, R.H., Blumberg, S.J., Pastor, P., Ghandour, R.M., Gfroerer, J.C., Hedden, S.L., Crosby, A.E., Visser, S.N., Schieve, L.A. *et al.* (2013) Mental health surveillance among children—United States, 2005–2011. *MMWR Surveill. Summ.*, **62**(Suppl 2), 1–35.
4. Aad, G., Abbott, B., Abdallah, J., Abdelalim, A.A., Abdesselam, A., Abdinov, O., Abi, B., Abolins, M., Abouzeid, O.S., Abramowicz, H. *et al.* (2012) Observation of a New chi_{b} State in Radiative Transitions to Upsilon(1S) and Upsilon(2S) at ATLAS. *Phys. Rev. Lett.*, **108**, 152001.
5. O'Roak, B.J., Deriziotis, P., Lee, C., Vives, L., Schwartz, J.J., Girirajan, S., Karakoc, E., Mackenzie, A.P., Ng, S.B., Baker, C. *et al.* (2011) Exome sequencing in sporadic autism spectrum disorders identifies severe de novo mutations. *Nat. Genet.*, **43**, 585–589.
6. Neale, B.M., Kou, Y., Liu, L., Ma'ayan, A., Samocha, K.E., Sabo, A., Lin, C.F., Stevens, C., Wang, L.S., Makarov, V. *et al.* (2012) Patterns and rates of exonic de novo mutations in autism spectrum disorders. *Nature*, **485**, 242–245.
7. Ku, C.S., Polychronakos, C., Tan, E.K., Naidoo, N., Pawitan, Y., Roukos, D.H., Mort, M. and Cooper, D.N. (2013) A new paradigm emerges from the study of de novo mutations in the context of neurodevelopmental disease. *Mol. Psychiatry*, **18**, 141–153.
8. Jiang, Y.H., Yuen, R.K., Jin, X., Wang, M., Chen, N., Wu, X., Ju, J., Mei, J., Shi, Y., He, M. *et al.* (2013) Detection of clinically relevant genetic variants in autism spectrum disorder by whole-genome sequencing. *Am. J. Hum. Genet.*, **93**, 249–263.
9. Steffenburg, S., Steffenburg, U. and Gillberg, C. (2003) Autism spectrum disorders in children with active epilepsy and learning disability:

comorbidity, pre- and perinatal background, and seizure characteristics. *Dev. Med. Child Neurol.*, **45**, 724–730.
10. Matsuo, M., Maeda, T., Sasaki, K., Ishii, K. and Hamasaki, Y. (2010) Frequent association of autism spectrum disorder in patients with childhood onset epilepsy. *Brain Dev.*, **32**, 759–763.
11. Saemundsen, E., Ludvigsson, P., Hilmarsdottir, I. and Rafnsson, V. (2007) Autism spectrum disorders in children with seizures in the first year of life—a population-based study. *Epilepsia*, **48**, 1724–1730.
12. Bolton, P.F., Carcani-Rathwell, I., Hutton, J., Goode, S., Howlin, P. and Rutter, M. (2011) Epilepsy in autism: features and correlates. *Br. J. Psychiatry*, **198**, 289–294.
13. Danielsson, S., Gillberg, I.C., Billstedt, E., Gillberg, C. and Olsson, I. (2005) Epilepsy in young adults with autism: a prospective population-based follow-up study of 120 individuals diagnosed in childhood. *Epilepsia*, **46**, 918–923.
14. Giovanardi Rossi, P., Posar, A. and Parmeggiani, A. (2000) Epilepsy in adolescents and young adults with autistic disorder. *Brain Dev.*, **22**, 102–106.
15. Lo-Castro, A. and Curatolo, P. (2013) Epilepsy associated with autism and attention deficit hyperactivity disorder: Is there a genetic link? *Brain Dev.*, pii: S0387-7604(13)00162-9.
16. Jerng, H.H., Pfaffinger, P.J. and Covarrubias, M. (2004) Molecular physiology and modulation of somatodendritic A-type potassium channels. *Mol. Cell. Neurosci.*, **27**, 343–369.
17. Bahring, R., Boland, L.M., Varghese, A., Gebauer, M. and Pongs, O. (2001) Kinetic analysis of open- and closed-state inactivation transitions in human Kv4.2 A-type potassium channels. *J. Physiol.*, **535**, 65–81.
18. Gebauer, M., Isbrandt, D., Sauter, K., Callsen, B., Nolting, A., Pongs, O. and Bahring, R. (2004) N-type inactivation features of Kv4.2 channel gating. *Biophys. J.*, **86**, 210–223.
19. Bahring, R. and Covarrubias, M. (2011) Mechanisms of closed-state inactivation in voltage-gated ion channels. *J. Physiol.*, **589**, 461–479.
20. Barghaan, J. and Bahring, R. (2009) Dynamic coupling of voltage sensor and gate involved in closed-state inactivation of kv4.2 channels. *J. Gen. Physiol.*, **133**, 205–224.
21. Lord, C., Rutter, M. and Le Couteur, A. (1994) Autism Diagnostic Interview–Revised: a revised version of a diagnostic interview for caregivers of individuals with possible pervasive developmental disorders. *J. Autism Dev. Disord.*, **24**, 659–685.
22. Lord, C., Rutter, M., DiLavore, P., Risi, S., Gotham, K. and Bishop, S. (2012) *Autism Diagnostic Observation Schedule, 2nd Edn: ADOS-2*. Western Psychological Services, Torrance, CA.
23. American Psychiatric Association. (2013) *Diagnostic and Statistical Manual of Mental Disorders*. 5th edn, American Psychiatric Association, Washington, DC.
24. Mullen, E.M. (1995) *Mullen Scales of Early Learning Manual*. American Guidance Service, Circle Pines, MN.
25. Jeon, D., Yang, Y.M., Jeong, M.J., Philipson, K.D., Rhim, H. and Shin, H.S. (2003) Enhanced learning and memory in mice lacking Na+/Ca2+ exchanger 2. *Neuron*, **38**, 965–976.
26. Kraus, M.R., Clauin, S., Pfister, Y., Di Maio, M., Ulinski, T., Constam, D., Bellanne-Chantelot, C. and Grapin-Botton, A. (2012) Two mutations in human BICC1 resulting in Wnt pathway hyperactivity associated with cystic renal dysplasia. *Hum. Mutat.*, **33**, 86–90.
27. Bouvrette, D.J., Price, S.J. and Bryda, E.C. (2008) K homology domains of the mouse polycystic kidney disease-related protein, Bicaudal-C (Bicc1), mediate RNA binding in vitro. *Nephron. Exp. Nephrol.*, **108**, e27–e34.
28. Birnbaum, S.G., Varga, A.W., Yuan, L.L., Anderson, A.E., Sweatt, J.D. and Schrader, L.A. (2004) Structure and function of Kv4-family transient potassium channels. *Physiol. Rev.*, **84**, 803–833.
29. Papazian, D.M., Timpe, L.C., Jan, Y.N. and Jan, L.Y. (1991) Alteration of voltage-dependence of Shaker potassium channel by mutations in the S4 sequence. *Nature*, **349**, 305–310.
30. Timpe, L.C., Schwarz, T.L., Tempel, B.L., Papazian, D.M., Jan, Y.N. and Jan, L.Y. (1988) Expression of functional potassium channels from Shaker cDNA in Xenopus oocytes. *Nature*, **331**, 143–145.
31. Long, S.B., Campbell, E.B. and Mackinnon, R. (2005) Crystal structure of a mammalian voltage-dependent Shaker family K+ channel. *Science*, **309**, 897–903.
32. Jerng, H.H., Kunjilwar, K. and Pfaffinger, P.J. (2005) Multiprotein assembly of Kv4.2, KChIP3 and DPP10 produces ternary channel complexes with ISA-like properties. *J. Physiol.*, **568**, 767–788.
33. Covarrubias, M., Bhattacharji, A., De Santiago-Castillo, J.A., Dougherty, K., Kaulin, Y.A., Na-Phuket, T.R. and Wang, G. (2008) The neuronal Kv4 channel complex. *Neurochem. Res.*, **33**, 1558–1567.
34. Wang, S., Patel, S.P., Qu, Y., Hua, P., Strauss, H.C. and Morales, M.J. (2002) Kinetic properties of Kv4.3 and their modulation by KChIP2b. *Biochem. Biophys. Res. Commun.*, **295**, 223–229.
35. Jerng, H.H., Dougherty, K., Covarrubias, M. and Pfaffinger, P.J. (2009) A novel N-terminal motif of dipeptidyl peptidase-like proteins produces rapid inactivation of KV4.2 channels by a pore-blocking mechanism. *Channels (Austin)*, **3**, 448–461.
36. Wang, H., Yan, Y., Liu, Q., Huang, Y., Shen, Y., Chen, L., Chen, Y., Yang, Q., Hao, Q., Wang, K. *et al.* (2007) Structural basis for modulation of Kv4 K+ channels by auxiliary KChIP subunits. *Nat. Neurosci.*, **10**, 32–39.
37. Jerng, H.H., Shahidullah, M. and Covarrubias, M. (1999) Inactivation gating of Kv4 potassium channels: molecular interactions involving the inner vestibule of the pore. *J. Gen. Physiol.*, **113**, 641–660.
38. Webster, S.M., Del Camino, D., Dekker, J.P. and Yellen, G. (2004) Intracellular gate opening in Shaker K+ channels defined by high-affinity metal bridges. *Nature*, **428**, 864–868.
39. Harpaz, Y., Gerstein, M. and Chothia, C. (1994) Volume changes on protein folding. *Structure*, **2**, 641–649.
40. Okamoto, N., Hatsukawa, Y., Shimojima, K. and Yamamoto, T. (2011) Submicroscopic deletion in 7q31 encompassing CADPS2 and TSPAN12 in a child with autism spectrum disorder and PHPV. *Am. J. Med. Genet. A*, **155A**, 1568–1573.
41. Scherer, S.W., Cheung, J., MacDonald, J.R., Osborne, L.R., Nakabayashi, K., Herbrick, J.A., Carson, A.R., Parker-Katiraee, L., Skaug, J., Khaja, R. *et al.* (2003) Human chromosome 7: DNA sequence and biology. *Science*, **300**, 767–772.
42. Mikhailov, A., Choufani, S., Skaug, J., Kolozsvari, D., Marshall, C., Scherer, S.W. and Vincent, J.B. Chromosomal translocation t(5;7)(q14;q31) and missense mutations implicate the voltage-gated potassium channel Kv4.2 gene, KCND2, on 7q31 in autism. *Presented at the Annual Meeting of The American Society of Human Genetics*, November, 2008, Philadelphia, PA.
43. Casey, J.P., Magalhaes, T., Conroy, J.M., Regan, R., Shah, N., Anney, R., Shields, D.C., Abrahams, B.S., Almeida, J., Bacchelli, E. *et al.* (2012) A novel approach of homozygous haplotype sharing identifies candidate genes in autism spectrum disorder. *Hum. Genet.*, **131**, 565–579.
44. Girirajan, S., Dennis, M.Y., Baker, C., Malig, M., Coe, B.P., Campbell, C.D., Mark, K., Vu, T.H., Alkan, C., Cheng, Z. *et al.* (2013) Refinement and discovery of new hotspots of copy-number variation associated with autism spectrum disorder. *Am. J. Hum. Genet.*, **92**, 221–237.
45. Br J PsychiatryMarshall, C.R., Noor, A., Vincent, J.B., Lionel, A.C., Feuk, L., Skaug, J., Shago, M., Moessner, R., Pinto, D., Ren, Y. *et al.* (2008) Structural variation of chromosomes in autism spectrum disorder. *Am. J. Hum. Genet.*, **82**, 477–488.
46. Kelleher, R.J. 3rd and Bear, M.F. (2008) The autistic neuron: troubled translation? *Cell*, **135**, 401–406.
47. Lee, H.Y., Ge, W.P., Huang, W., He, Y., Wang, G.X., Rowson-Baldwin, A., Smith, S.J., Jan, Y.N. and Jan, L.Y. (2011) Bidirectional regulation of dendritic voltage-gated potassium channels by the fragile X mental retardation protein. *Neuron*, **72**, 630–642.
48. Darnell, J.C., Van Driesche, S.J., Zhang, C., Hung, K.Y., Mele, A., Fraser, C.E., Stone, E.F., Chen, C., Fak, J.J., Chi, S.W. *et al.* (2011) FMRP stalls ribosomal translocation on mRNAs linked to synaptic function and autism. *Cell*, **146**, 247–261.
49. Kim, E. and Hoffman, D.A. (2012) Dynamic regulation of synaptic maturation state by voltage-gated A-type K+ channels in CA1 hippocampal pyramidal neurons. *J. Neurosci.*, **32**, 14427–14432.
50. Parikshak, N.N., Luo, R., Zhang, A., Won, H., Lowe, J.K., Chandran, V., Horvath, S. and Geschwind, D.H. (2013) Integrative functional genomic analyses implicate specific molecular pathways and circuits in autism. *Cell*, **155**, 1008–1021.
51. McKenna, A., Hanna, M., Banks, E., Sivachenko, A., Cibulskis, K., Kernytsky, A., Garimella, K., Altshuler, D., Gabriel, S., Daly, M. *et al.* (2010) The Genome Analysis Toolkit: a MapReduce framework for analyzing next-generation DNA sequencing data. *Genome Res.*, **20**, 1297–1303.
52. DePristo, M.A., Banks, E., Poplin, R., Garimella, K.V., Maguire, J.R., Hartl, C., Philippakis, A.A., del Angel, G., Rivas, M.A., Hanna, M. *et al.* (2011)

A framework for variation discovery and genotyping using next-generation DNA sequencing data. *Nat. Genet.*, **43**, 491–498.
53. Bahlo, M. and Bromhead, C.J. (2009) Generating linkage mapping files from Affymetrix SNP chip data. *Bioinformatics*, **25**, 1961–1962.
54. Smith, K.R., Bromhead, C.J., Hildebrand, M.S., Shearer, A.E., Lockhart, P.J., Najmabadi, H., Leventer, R.J., McGillivray, G., Amor, D.J., Smith, R.J. *et al.* (2011) Reducing the exome search space for mendelian diseases using genetic linkage analysis of exome genotypes. *Genome Biol.*, **12**, R85.
55. Purcell, S., Neale, B., Todd-Brown, K., Thomas, L., Ferreira, M.A., Bender, D., Maller, J., Sklar, P., de Bakker, P.I., Daly, M.J. *et al.* (2007) PLINK: a tool set for whole-genome association and population-based linkage analyses. *Am. J. Hum. Genet.*, **81**, 559–575.